Progress In Electromagnetics Research C, Vol. 37, 199–209, 2013

A COMPREHENSIVE STUDY ON DECOUPLING BETWEEN INVERTED-F ANTENNAS USING SLITTED GROUND PLANE

Takeshi Fukusako* **and Yasuhiro Harada**

Kumamoto University, 2-39-1, Kurokami, Chuo-ku, Kumamoto 860-8555, Japan

Abstract—A simple structure for achieving a low mutual coupling between two inverted-F antennas is presented. The low coupling between the antennas is obtained by using two slits on the ground plane. As a result, the interval between the antennas can be shorter than $\lambda/8$. Furthermore, this technique can be combined with other techniques. This is good for designing small handsets which allow shorter intervals between antennas. In this paper, the authors present a slitted ground structure and consider the mechanism of the structure where a mutual coupling of $-35\,\mathrm{dB}$ can be achieved using the slitted ground plane.

1. INTRODUCTION

High-speed mobile telecommunications with wireless technologies have been getting popular in recent years. In those technologies, such as MIMO (Multiple-Input Multipule-Output) or LTE (Long Term Evolution), antennas should be arrayed with a low mutual coupling so as to achieve sufficient channel capacity. Several techniques have been presented to reduce mutual coupling between antenna elements, i.e. decoupling, at around the resonance frequency. In [1–4], the EBG (Electromagnetic Band Gap) structures or metasurfaces have been installed between antenna elements. Using coupling elements is another technique to reduce the coupling [5, 6]. Installing a network is also a good candidate [7]. In addition to this, neutralization techniques have been proposed [8–11]. In those technologies, two antenna elements are connected with a metallic line or circuits for decoupling the antennas.

Received 14 January 2013, Accepted 16 February 2013, Scheduled 18 February 2013

* Corresponding author: Takeshi Fukusako (fukusako@cs.kumamoto-u.ac.jp).

As mentioned above, several types of techniques for decoupling have been proposed. However, most of them require a complicated procedure to design. Having slots or slits on the ground plane is a simple and effective technique for reducing the mutual coupling [12–14]. In [12], slot stubs in the ground plane have been arrayed so as to make a band rejection filter to check the current on the ground plane. As shown in [13], control of the current on the ground using a slot is effective to reduce the coupling. In [14], two parallel slots resonated with a length of $\lambda/2$ are installed to reduce the coupling.

Considering the simplicity of slitted ground structures, the authors propose a slitted structure with $\lambda/2$ and discuss results of comprehensive studies on the decoupling mechanism in the slitted ground structure. This technique also controls the current on the ground. The consideration about this behavior may give a hint to advance and design other decoupling structures. Moreover, the slitted ground structure can be combined with other techniques for decoupling [15]. This is a merit of the slitted structure for enhancing the decoupling between antennas with shorter intervals.

2. STRUCTURE

Figure 1 shows the geometry of the proposed array structure. The structure consists of two inverted-F antenna elements and a slitted ground plane with a fixed dimension of 40 mm × 100 mm × 0.3 mm. The ground plane are slitted with two slits having dimensions of L_s (= 73 mm = $\lambda/2$) × L_x and L_{s2} (= 20 mm) × L_x. In other words, each inverted F antenna with a ground plane has been connected with a short line having a dimension of L_x = 6 mm × L_y = 7 mm. This short line is installed at a position of L_s from the ground edge by the antenna elements. A test frequency of 2 GHz is chosen, and an antenna interval of g is basically fixed at $\lambda/8$ for the test frequency. In the following sections, Ansoft HFSS ver.11 has been used for obtaining the simulated results.

3. EFFECT OF THE SLITTED GROUND STRUCTURE

The effect of the slitted structure is compared among three cases. For case (a), the two antennas are installed on a non-slitted ground plane with the dimension of 40 mm × 100 mm × 0.3 mm. For case (b), each antenna has a separated ground plane where the connecting short line shown in Figure 1 has been removed. Furthermore, case (c) is the proposed structure which has been shown in the Figure 1 with the slitted ground plane.

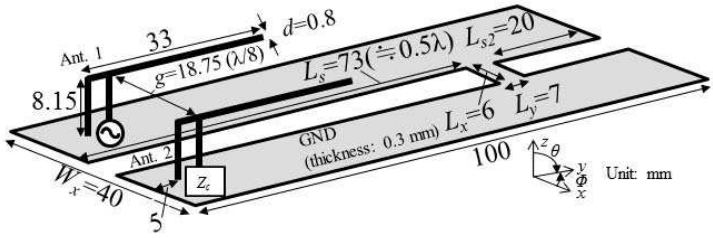

Figure 1. Geometory of the proposed inverted-F antenna array.

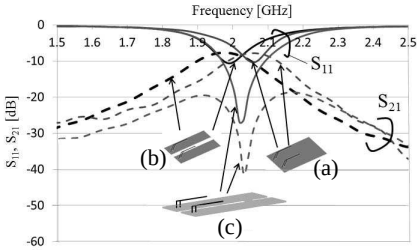

Figure 2. The effect of the ground structures.

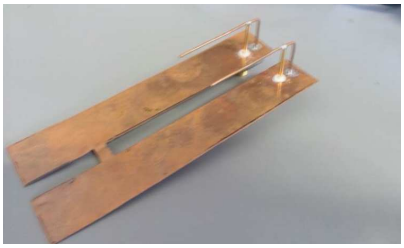

Figure 3. Photograph of the fabricated structure.

The simulated S_{11} characteristics and simulated S_{21}, the coupling between the antennas, are shown in Figure 2 where the three cases are also shown. From the results, only case (c) shows the decoupling effect with the minimized S_{21} at around 2.05 GHz where the sufficient matching to 50 Ω are achieved. In other cases, (a) and (b), the S_{21} characteristics show coupling with a peak of each curve at around the frequencies where the S_{11} characteristics are minimized. As a result, we can find that the slitted (or connected) ground structure (c) is effective for decoupling between the antennas.

The simulated results for case (c) are compared with measured results. Figure 3 is a photograph of the fabricated structure, where all dimensions are the same as those in Figure 1. In this figure, the metallic materials are copper, and SMA connectors (not shown in the photo) are installed behind the ground.

Figure 4 shows the simulated and measured S_{11} and S_{21} characteristics of the proposed structure (case (c)). Around the frequency band where $|S_{11}| < -10$ dB, we can observe the decoupling effect in the measurement showing a good agreement with the simulated results. However, the measured S_{21} is higher than the

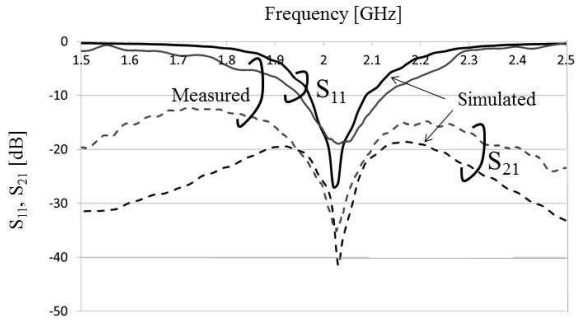

Figure 4. The simulated and measured S_{11} and S_{21} characteristics.

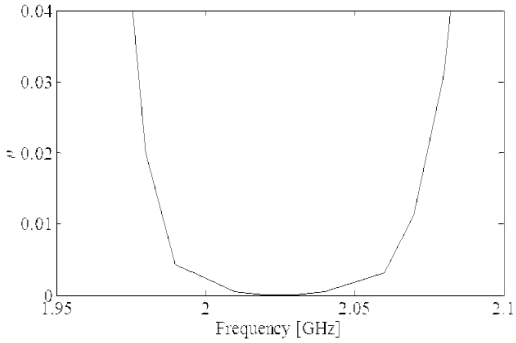

Figure 5. Simulated correlation coefficient.

simulated ones except this decoupling frequency, because of the coupling between the coaxial cables connected to the feed points, respectively.

The antenna correlation is an important parameter for evaluating MIMO antennas. There are two well-known approaches for calculating the correlation. One is based on the radiation pattern in the far field [16], and the other is based on the S-parameters obtained at the antenna terminals [17, 18]. In this paper, the antenna correlation ρ is calculated based on the latter method using S-parameters as follows:

$$\rho = \frac{|S_{11}^* S_{12} + S_{21}^* S_{22}|^2}{(1 - |S_{11}|^2 - |S_{21}|^2)(1 - |S_{22}|^2 - |S_{12}|^2)}, \tag{1}$$

where the $*$ mark denotes the complex conjugate. In this equation, $S_{11} = S_{22}$ and $S_{21} = S_{12}$ can be assumed for the present structure.

For the proposed structure, Figure 5 shows the simulated correlation coefficient ρ with respect to frequency. At the resonant

frequency around 2.05 GHz, the simulated ρ is much smaller than 0.001. This antenna system is available for the frequency from approximately 1.98 GHz to 2.08 GHz (simulated $|S_{11}| < -10$ dB). In this frequency range, ρ value is less than 0.04. This behavior shows sufficiently low correlation referencing the discussions in [16–19].

4. DECOUPLING MECHANISM

4.1. Parametric Studies

For understanding the decoupling mechanism in the proposed structure, this section provides, at first, some parametric studies where default structural parameters are assumed as shown in Figure 1 except the variable parameter.

Figure 6 shows the effect of slit length L_s. With an increase in L_s from 71 mm to 75 mm, decoupling frequency with minimized S_{21} is shifted higher. In addition, S_{21} is minimized maximally when

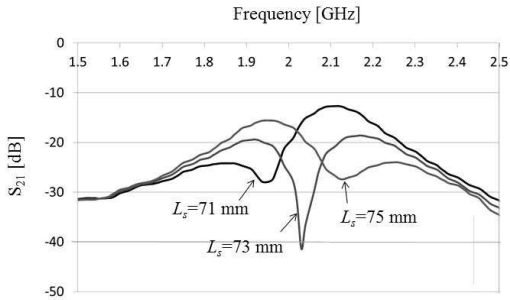

Figure 6. Variation in decoupling effect with L_s.

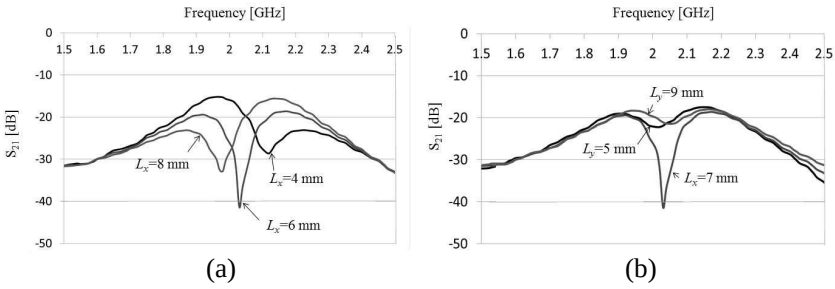

Figure 7. Effect of the dimensions of the connecting short line, (a) is the effec of L_x, and (b) is the effect of L_y.

$L_s = 73\,\text{mm}$ corresponding to $\lambda/2$. As a result, the L_s should be chosen as around $\lambda/2$ for obtaining an effective decoupling effect.

The effects of dimensions in the connecting short line L_x and L_y are presented as shown in Figures 7(a) and (b). According to the results, we can see that there is the most suitable value on each parameter. These dimensions are related to the current density on the short line, in other words, these dimensions decide the impedance at the end of the longer slit with L_s. As mentioned above, we can conclude that the decoupling effect is related to the dimensions of L_s, L_x and L_y.

4.2. Current and Field Distributions

For further discussions, a current distribution at respective resonant frequency is shown in Figure 8 for structures (a), (b) and (c) in Figure 2. In these figures, the antenna 1 on the left is fed, but the antenna 2 on the right is terminated by a 50-Ω load at the feeding point.

Strong current from antenna 1 reaches antenna 2 in structure (a), which results in the coupling between the antennas. In structure (b), the current on the left ground with antenna 1 is concentrating on both ground edges. On the other ground with antenna 2, strong current is coupled with the current on the left ground flowing in the opposite direction along the left edge. This current on the right ground leads

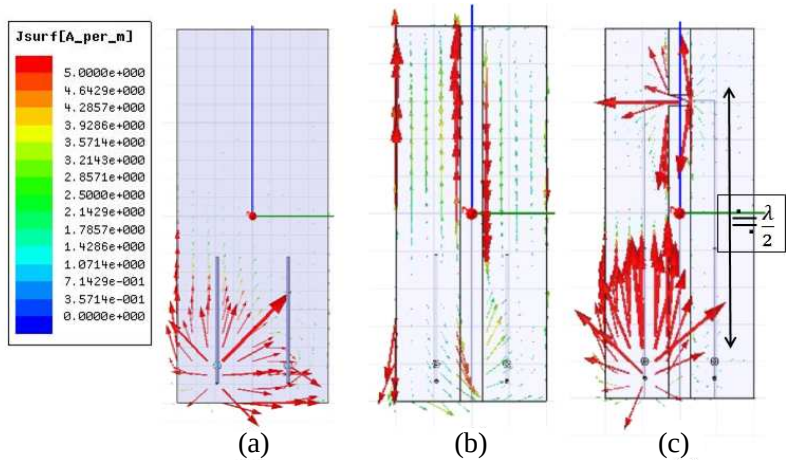

Figure 8. Current distribution on (a) the common ground for the antennas, (b) the separated grounds, and (c) the proposed slitted ground structure.

to the coupling between both antennas.

On the other hand, structure (c) shows a different behavior. Strong current can be observed on the connecting short line in addition to antenna 1. The short line has a narrow width so that the current can concentrate here with high density. Considering the slit length of $\lambda/2$, current must be concentrated along two lines. One is the connecting short line. This connecting line is located too far from the antennas to couple them. The other line must be an assumed straight line connecting the feed points of the antennas; however, there is no such a metallic line in the slit. Therefore, mutual coupling between the antennas can be avoided since strong current path to connect the antennas cannot exist on the grounds.

For making further comprehension, the difference between

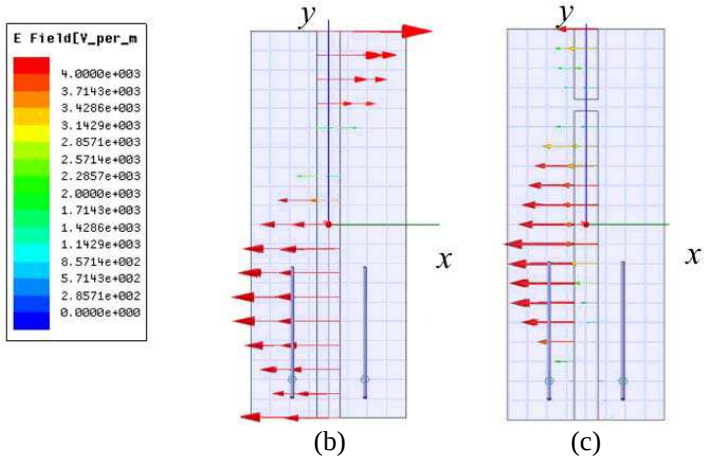

Figure 9. Distribution of electric field in the slits with (b) the separated grounds and (c) the slitted ground structure.

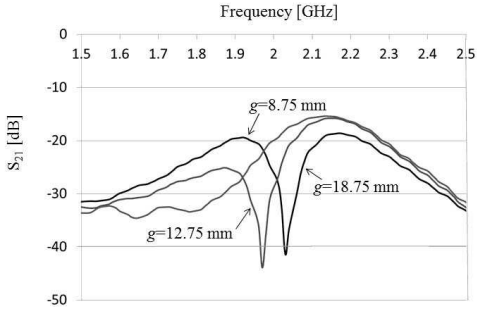

Figure 10. Variation in coupling characteristics with g.

structures (b) and (c) in Figure 8 can be discussed with regard to the electric field (e-field). Figure 9 shows the distributions of electric field in the slit. In both structures, the e-fields have a sinusoidal distribution of strength with respect to the y direction. However, in structure (b) with the separated grounds, strong e-field can be observed in the vicinity of the two antennas. This indicates that the two antennas can be coupled capacitively.

In structure (c), e-field is weak around the feed points since the feed points are located having a distance of $\lambda/2$ from the short line. We can conclude that this behavior around the feed points also yields the decoupling effect.

Finally, the interval g between the antenna is analyzed. Figure 10

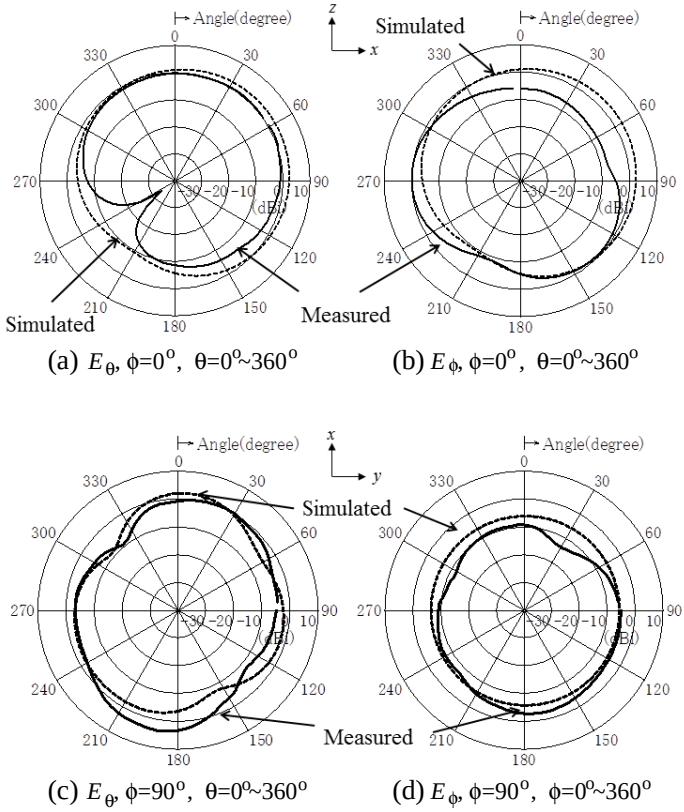

Figure 11. Radiation patterns, where solid lines show measured results, and dotted line show simulated results, (a) and (b) are in the z-x plane, and (c) and (d) are in the x-y plane.

shows the variation in S_{21} with g. In this paper, g has been basically fixed as $\lambda/8$ in all discussions. According to the figure, the coupling is still low when $g = 12.75\,\text{mm}$ ($< 0.1\lambda$). However, when g is around $8.75\,\text{mm}$ ($\simeq 0.058\lambda$), the coupling has not been suppressed sufficiently.

5. RADIATION PATTERNS

Radiation patterns at the resonant frequency are simulated and measured. The results are shown in Figure 11. In the measurement, antenna 1 in Figure 1 is fed by a coaxial cable, and the feeding point of antenna 2 is terminated with a 50-Ω load. Although we have installed a balun on the feeding cable during all experiments in this paper, the radiation patterns have been affected by the current on the coaxiation cable for this size of the ground plane. Therefore, as seen in Figures 11(a) and (b), we can see a little difference between the simulated and measured results. In addition to this, the fabrication error of the inverted-F antenna may be another reason for the difference. However, in Figures 11(c) and (d), good agreements can be observed between the simulated and measured results.

6. CONCLUSIONS

A decoupling technique between antennas using a slitted ground structure has been presented and analyzed. This structure has a merit that it could be minimized furthermore using a meandered slit on the ground. Moreover, even for a narrower interval between antenna elements, sufficiently low coupling may be achieved using a combination of the presented principle with another decoupling technique. As a result, we can expect antenna arrays with low coupling in smaller structures for handsets or terminals. The analyzed results may give a good hint in developing other decoupling techniques.

ACKNOWLEDGMENT

The authors would like to appreciate Japan Society for the Promotion of Science (JSPS) with Grants-in-aid for Scientific Research Program.

REFERENCES

1. Xin, H., K. Matsugatani, M. Kim, J. Hacker, J. A. Higgins, M. Rosker, and M. Tanaka, "Mutual coupling reduction of low-profile monopole antennas on high-impedance ground plane," *Electronics Letters*, Vol. 38, No. 16, 849–850, Aug. 2002.

2. Yang, F. and Y. Rahmat-Samii, "Microstrip antennas integrated with electromagnetic band-gap (EBG) structures: A low mutual coupling design for array application," *IEEE Trans. Antennas Propag.*, Vol. 51, No. 10, 2936–2946, Oct. 2003.
3. Buell, K., H. Mosallaei, and K. Sarabandi, "Metamaterial insulator enabled surperdirective array," *IEEE Trans. Antennas Propag.*, Vol. 55, No. 4, 1074–1085, Apr. 2007
4. Saenz, E., I. Ederra, R. Gonzalo, S. Pivnenko, O. Breinbjerg, and P. de Maagt, "Coupling reduction between dipole antenna elements by using a planar meta-surface," *IEEE Trans. Antennas Propag.*, Vol. 57, No. 2, 383–394, Feb. 2009.
5. Mak, A. C. K., C. R. Rowell, and R. D. Murch, "Isolation enhancement between two closely packed antennas," *IEEE Trans. Antennas Propag.*, Vol. 56, No. 11, 3411–3419, Nov. 2008.
6. Song, Y. J. and K. Sarabandi, "Suppression of the mutual coupling two adjacent miniaturized antennas utilizing printed resonant circuits," *IEEE Int. Symp. Antennas and Propag. and URSI/URSI National Radio Science Meeting*, 1–4, Charleston, USA, Jun. 2009.
7. Chen, S. C., Y. S. Wang, and S. J. Chung, "A decoupling technique for increasing the port isolation between two strongly coupled antennas," *IEEE Trans. Antennas Propag.*, Vol. 56, No. 12, 3650–3658, Dec. 2008.
8. Diallo, A., C. Luxey, P. L. Thuc, R. Staraj, and G. Kossiavas, "Study and reduction of the mutual coupling between two mobile phone PIFAs operating in the DCS1800 and UMTS bands," *IEEE Trans. Antennas Propag.*, Vol. 54, No. 11, 3063–3074, Nov. 2006.
9. Diallo, A., C. Luxey, P. L. Thuc, R. Staraj, and G. Kossiavas, "Enhanced two-antenna structures for universal mobile telecommunications system diversity terminals," *IET Microw. Antennas Propag.*, Vol. 2, 93–101, 2008.
10. Itoh, J., N. T. Hung, and H. Morishita, "The mutual coupling reduction between two J-shaped folded monopole antennas for handset," *IEICE Trans. Commun.*, Vol. E94-B, No. 5, 1161–1167, May 2011.
11. Su, S. W., C. T. Lee, and F. S. Chang, "Printed MIMO-antenna system using neutralization-line technique for wireless USB-dongle applications," *IEEE Trans. Antennas Propag.*, Vol. 60, No. 2, 456–463, Feb. 2012.
12. Chiu, C. Y., C. H. Cheng, R. D. Murch, and C. R. Rowell, "Reduction of mutual coupling between closely-packed antenna elements," *IEEE Trans. Antennas Propag.*, Vol. 55, No. 6, 1732–

1738, Jun. 2007.

13. Zhang, S., S. Naeem, and S. He, "Reducing mutual coupling for an extremely closely-packed tunable dual-element PIFA array through a resonant slot antenna formed in-between," *IEEE Trans. Antennas Propag.*, Vol. 58, No. 8, 2771–2776, Jun. 2007.
14. Sonkki, M. and E. Salonen, "Low mutual coupling between monopole antennas by using two $\lambda/2$ slots," *IEEE Antennas and Wireless Propag. Lett.*, Vol. 9, 138–141, 2010.
15. Jolani, F., A. M. Dadgarpour, and G. Dadashzadeh, "Reduction of mutual coupling between dual-element antennas with new PBG techniques," *13th Int. Symp. on Antenna Technology and Applied Electromagnetics and the Canadian Radio Sciences Meeting*, 1–4, Banff, Canada, Feb. 2009.
16. Kim, Y., T. Hayashi, Y. Koyanagi, and H. Morishita, "Compact built-in handset MIMO antenna using L-shaped folded monopole antennas," *IEICE Trans. Commun.*, Vol. E91-B, No. 6, 1743–1751, Jun. 2008.
17. Thaysen, J. and K. B. Jakobsen, "Envelope correlation in (N, N) MIMO antenna array from scattering parameters," *Microwave and Optical Technology Letters*, Vol. 48, No. 5, 832–834, May 2006.
18. Najam, A., Y. Duroc, and S. Tedjni, "UWB-MIMO antenna with novel stub structure," *Progress In Electromagnetic Research C*, Vol. 19, 245–257, 2011.
19. Sharawi, M. S., A. B. Numan, and D. N. Aloi, "Isolation improvement in a dual-band dual-element MIMO antenna system using capacitively loaded loops," *Progress In Electromagnetic Research*, Vol. 134, 247–266, 2013.